

Distribution of the dissipated angular momentum in heavy-ion collisions

J. Q. Li* and G. Wolschin

Max-Planck-Institut für Kernphysik, Heidelberg, Federal Republic of Germany

(Received 29 September 1982)

The angular-momentum distributions of both fragments in low-energy heavy-ion collisions are calculated in a nonequilibrium-statistical model. The distribution functions are obtained analytically via moment expansion on the basis of a transport equation. They include the correlations between the two fragments. In conjunction with a phenomenological model for the description of the relative motion we compute fragment angular-momentum distributions as a function of energy loss and compare with experimental data.

NUCLEAR REACTIONS Deeply inelastic heavy-ion collisions. Calculated angular-momentum distributions of both fragments. Comparison with γ -multiplicity data.

I. INTRODUCTION

Nonequilibrium-statistical concepts have proven to be successful tools for the understanding of dissipative processes in low-energy heavy-ion collisions. Phenomenological models based on transport equations have been introduced to describe the transfer of mass or charge between the fragments, and the transport of angular momentum from relative motion to intrinsic excitation.¹⁻⁴ In both cases the statistical fluctuations associated with the dissipative processes are the outstanding features of the observables. However, whereas the widths of the mass or element distributions are directly accessible experimentally, only indirect evidence exists for the relevance of statistical fluctuations in the distributions of angular momenta in the fragments. They are most pronounced in the completely damped energy-loss domain where equilibrium-statistical models start to be valid.⁵ An indication of the importance of angular-momentum fluctuations⁶ is given through the flatness of γ -multiplicity distributions⁷ and the loss of alignment⁸ at large energy loss where the fluctuations dominate the mean value of the dissipated angular momentum. The simultaneous fluctuations in energy loss for fixed impact parameter complicate the picture since they wash out the fall of the alignment at large Q value.⁹

In detailed comparisons with experimental data, it is necessary that the calculations provide the angular-momentum distributions of both fragments, with the correlations properly taken into account. Some results of an analytical treatment of the correlations in a nonequilibrium-statistical model have been reported in Ref. 10. In the current work we give the complete calculation on the basis of a

Fokker-Planck equation for the angular-momentum distributions of both fragments. The differential equations for first and second moments of the fragment angular momentum are derived and solved analytically in Sec. II. The coupling to the relative motion of the fragments is considered in Sec. III. Applications of the model to several reactions are given in Sec. IV. Comparison with data from a γ -multiplicity measurement¹¹ is done for $^{86}\text{Kr} + ^{154}\text{Sm}$, whereas results for $^{208}\text{Pb} + ^{238}\text{U}$ may be of interest for a forthcoming double-sequential fission experiment.¹² The conclusions are drawn in Sec. V.

II. DERIVATION AND SOLUTION OF THE MOMENT EQUATIONS

In contrast to previous nonequilibrium-statistical approaches⁶ we consider the intrinsic angular momenta \vec{I}_k ($k=1,2$) of the two fragments as independent variables. Hence the correlation of the corresponding distributions will be properly included in the treatment. The distribution function $P(\vec{I}_1, \vec{I}_2; t)$ of the respective fragment angular momenta \vec{I}_1, \vec{I}_2 obeys a transport equation of the Fokker-Planck-type

$$\frac{\partial P}{\partial t} = - \sum_{i,k} \frac{\partial}{\partial I_k^i} (v_k P) + \sum_{i,j,k,k'} \frac{\partial^2}{\partial I_k^i \partial I_{k'}^j} (D_{kk'}^{ij} P). \quad (2.1)$$

We do not consider the relative motion explicitly at this stage. Its treatment would give rise to inertial and potential terms in (2.1), whereas here only the statistical process of angular-momentum dissipation is considered. The description of the relative motion

that is necessary for applications will be given in the following section. The angular-momentum diffusion tensor \vec{D} is given by a 6×6 matrix with components $D_{kk'}^{ij}$ corresponding to the fragments $k, k' = 1, 2$ and spatial directions $i, j = 1, 2, 3$. We take the initial relative angular momentum $\vec{I} = (0, 0, I)$ to define the z direction. Nonvanishing in-plane components of the angular-momentum diffusion tensor in the x and y directions cause a misalignment^{5,6,8} of the dissipated angular momentum. Owing to the geometry of the composite system, these components are generally different¹³ from those in the z direction, and consequently the magnitude of the fluctuations differs in the spatial directions. This effect has also been investigated numerically in a complementary model where quantum fluctuations associated with elementary modes of excitation generate angular-momentum fluctuations.¹⁴ Here we focus on an analytical treatment of the statistical fluctuations. To be able to solve the transport equation (2.1) in closed form, however, simplifications of the diffusion tensor are necessary. We take the spatial components of the diffusion tensor in both fragments to be equal. Hence, differences in the in-plane fluctuations which become important, especially at large mass asymmetry, cannot be described. In addition, the mixed components of the diffusion tensor are neglected such that the model is essentially determined by the diffusion coefficients D_1, D_2 referring to the two fragments.

The components v_k ($k = 1, 2$) of the angular-momentum drift vector are related⁶ to the diffusion coefficients D_k via the fragment temperature

$$T_k^{(l)} = (E_k^{(l)} / a_k)^{1/2}$$

with the excitation energy $E_k^{(l)}$ and the level-density parameter $a_k = A_k / 10$ and $D_{kk} \equiv D_k$

$$P(\vec{I}_1, \vec{I}_2; t) = (2\pi)^{-3} d^{-3/2} \exp \left[-\frac{(\vec{I}_1 - \langle \vec{I}_1 \rangle)^2 \sigma_2^2}{2d} - \frac{(\vec{I}_2 - \langle \vec{I}_2 \rangle) \sigma_1^2}{2d} + \frac{(\vec{I}_1 - \langle \vec{I}_1 \rangle)(\vec{I}_2 - \langle \vec{I}_2 \rangle) \sigma_{12}^4}{d} \right] \quad (2.5)$$

where

$$d = \sigma_1^2 \sigma_2^2 - \sigma_{12}^4. \quad (2.6)$$

The mean values of the fragment angular momenta remain in the (positive or negative) z direction at all times, $\langle \vec{I}_k \rangle = (0, 0, \langle I_k^z \rangle)$. In-plane components of the angular momentum are generated by statistical fluctuations only. We obtain for the differential equations of the mean values

$$\frac{d}{dt} \langle I_1^z \rangle = a_1 \langle I_1^z \rangle + b_1 \langle I_2^z \rangle + c_1, \quad (2.7)$$

$$v_k^{(l)} = -\frac{D_k^{(l)}}{T_k^{(l)}} \frac{\partial U_l}{\partial I_k}. \quad (2.2)$$

The average excitation energy $E^{(l)}$ will be calculated for each initial relative angular momentum l in a model that describes the relative motion. It is assumed to be shared between the two fragments in proportion to the mass such that the fragment temperatures for each l value are equal. The centrifugal part of the driving potential is

$$U_l = \frac{I_1^2}{2\mathcal{J}_1} + \frac{I_2^2}{2\mathcal{J}_2} + \frac{(\vec{I} - \vec{I}_1 - \vec{I}_2)^2}{2\mathcal{J}_{\text{rel}}}, \quad (2.3)$$

with the respective intrinsic and relative moments of inertia $\mathcal{J}_k, \mathcal{J}_{\text{rel}}$ which we calculate in the rigid-body approximation. The correlations in the angular-momentum distributions of the two fragments, as imposed by overall angular-momentum conservation

$$\vec{I} = \vec{I}_1 + \vec{I}_2 + \vec{I}_f, \quad (2.4)$$

enter the model through the centrifugal part of the driving potential and thus, through the drift coefficient. The less important correlations due to the off-diagonal components of the diffusion tensor will not be considered. We solve (2.1) for each initial l value for fixed $D_1^{(l)}, D_2^{(l)}$ with $v_1^{(l)}, v_2^{(l)}$ being linearly dependent on the variables according to (2.2) and (2.3). We derive coupled differential equations for the mean values $\langle \vec{I}_k \rangle$, variances

$$\sigma_k^2 = \langle I_k^2 \rangle - \langle \vec{I}_k \rangle^2$$

and covariance

$$\sigma_{12}^2 = \langle \vec{I}_1 \vec{I}_2 \rangle - \langle \vec{I}_1 \rangle \langle \vec{I}_2 \rangle.$$

They define Gaussian solutions

$$\frac{d}{dt} \langle I_2^z \rangle = a_2 \langle I_2^z \rangle + b_2 \langle I_1^z \rangle + c_2.$$

The initial condition is taken as $\langle I_1^z \rangle = \langle I_2^z \rangle = 0$ for $t = 0$ since a finite fragment spin in the ground state is usually negligible compared to the large amounts of angular momentum generated in the fragments during the reaction. We derive the coupled equations for the variances as

$$\frac{d}{dt} \vec{\sigma}^2 = M \vec{\sigma}^2 + \vec{D}, \quad (2.8)$$

where

$$\vec{\sigma}^2 \equiv \begin{pmatrix} \sigma_1^2 \\ \sigma_2^2 \\ \sigma_{12}^2 \end{pmatrix}, \quad \vec{D} \equiv 2 \begin{pmatrix} D_1 \\ D_2 \\ 0 \end{pmatrix} \quad (2.9)$$

and

$$M = \begin{pmatrix} 2a_1 & 0 & 2b_1 \\ 0 & 2a_2 & 2b_2 \\ b_2 & b_1 & (a_1 + a_2) \end{pmatrix} \quad (2.10)$$

with

$$a_k = -\frac{D_k}{T} \left[\frac{\mathcal{J}_{\text{rel}} + \mathcal{J}_k}{\mathcal{J}_{\text{rel}} \mathcal{J}_k} \right],$$

$$b_k = -\frac{D_k}{T} \frac{1}{\mathcal{J}_{\text{rel}}}, \quad (2.11)$$

$$c_k = -\frac{D_k}{T} \frac{l}{\mathcal{J}_{\text{rel}}}.$$

We have abbreviated $T \equiv T_k^{(l)}$ and $D_k \equiv D_k^{(l)}$. The initial conditions for the variances are $\sigma_1^2 = \sigma_2^2 = \sigma_{12}^2 = 0$ at $t=0$. We solve the coupled equations via Laplace transformation. The analytical results are ($k=1,2$)

$$\langle I_k^2 \rangle = \frac{\mathcal{J}_k}{\mathcal{J}_{\text{tot}}} l - A_k \exp(-t/\tau_1) - B_k \exp(-t/\tau_2) \quad (2.12)$$

with

$$A_{1,2} = \left[\frac{D_{2,1}}{\lambda_1 \mathcal{J}_{2,1} T} + 1 \right] \frac{D_{1,2}}{(\lambda_2 - \lambda_1) \mathcal{J}_{\text{rel}} T} l,$$

$$B_{1,2} = \left[\frac{D_{2,1}}{\lambda_2 \mathcal{J}_{2,1} T} + 1 \right] \frac{D_{1,2}}{(\lambda_1 - \lambda_2) \mathcal{J}_{\text{rel}} T} l, \quad (2.13)$$

and

$$\lambda_{1,2} = \frac{1}{2T \mathcal{J}_{\text{rel}}} \left\{ -\frac{D_1}{\mathcal{J}_1} (\mathcal{J}_1 + \mathcal{J}_{\text{rel}}) - \frac{D_2}{\mathcal{J}_2} (\mathcal{J}_2 + \mathcal{J}_{\text{rel}}) \right. \\ \left. \pm \left[\frac{D_1^2}{\mathcal{J}_1^2} (\mathcal{J}_1 + \mathcal{J}_{\text{rel}})^2 + \frac{D_2^2}{\mathcal{J}_2^2} (\mathcal{J}_2 + \mathcal{J}_{\text{rel}})^2 + 4D_1 D_2 \right. \right. \\ \left. \left. - \frac{2D_1 D_2}{\mathcal{J}_1 \mathcal{J}_2} (\mathcal{J}_1 + \mathcal{J}_{\text{rel}})(\mathcal{J}_2 + \mathcal{J}_{\text{rel}}) \right]^{1/2} \right\}. \quad (2.14)$$

The total moment of inertia is $\mathcal{J}_{\text{tot}} = \mathcal{J}_{\text{rel}} + \mathcal{J}_1 + \mathcal{J}_2$. For each impact parameter, two relaxation times $\tau_{1,2} = -1/\lambda_{1,2}$ appear according to the two degrees of freedom taken into account in our model. For the variances we obtain

$$\sigma_1^2 = \frac{\mathcal{J}_1 (\mathcal{J}_{\text{rel}} + \mathcal{J}_2)}{\mathcal{J}_{\text{tot}}} T + E_1 \exp[-2t/\tau_1] - F_1 \exp[-2t/\tau_2], \quad (2.15)$$

$$\sigma_2^2 = \frac{\mathcal{J}_2 (\mathcal{J}_{\text{rel}} + \mathcal{J}_1)}{\mathcal{J}_{\text{tot}}} T + E_2 \exp[-2t/\tau_1] - F_2 \exp[-2t/\tau_2],$$

where

$$E_{1,2} = \frac{D_{1,2} [\lambda_1 \mathcal{J}_{\text{rel}} \mathcal{J}_{1,2} T + D_{2,1} (\mathcal{J}_{\text{rel}} + \mathcal{J}_{2,1})]}{\lambda_1 (\lambda_1 - \lambda_2) \mathcal{J}_{\text{rel}} \mathcal{J}_{2,1} T}, \quad (2.16)$$

$$F_{1,2} = \frac{D_{1,2} [\lambda_2 \mathcal{J}_{2,1} \mathcal{J}_{\text{rel}} T + D_{1,2} (\mathcal{J}_{\text{rel}} + \mathcal{J}_{2,1})]}{\lambda_2 (\lambda_1 - \lambda_2) \mathcal{J}_{\text{rel}} \mathcal{J}_{2,1} T}.$$

Finally the covariance is

$$\sigma_{12}^2 = -\frac{\mathcal{J}_1 \mathcal{J}_2}{\mathcal{J}_{\text{tot}}} T - \frac{D_1 D_2}{\lambda_1 (\lambda_1 - \lambda_2) \mathcal{J}_{\text{rel}} T} \exp[-2t/\tau_1] \\ + \frac{D_1 D_2}{\lambda_2 (\lambda_1 - \lambda_2) \mathcal{J}_{\text{rel}} T} \exp[-2t/\tau_2]. \quad (2.17)$$

It is negative for all times, and hence the distributions of the intrinsic angular momenta in the two fragments are anticorrelated.¹⁰

The results at statistical equilibrium follow from these equations for $t \gg \tau_1, \tau_2$. For the mean values, the equilibrium result is given in terms of the stick-

ing limit

$$\langle I_k \rangle_{\text{equ}} = l \cdot \mathcal{J}_k / \mathcal{J}_{\text{tot}} \quad (2.18)$$

and for the sum of the mean values we recover the result⁶

$$\langle I \rangle_{\text{equ}} = l(\mathcal{J}_1 + \mathcal{J}_2) / \mathcal{J}_{\text{tot}} \quad (2.19)$$

In the formulation of Ref. 6, we have been dealing with the fluctuations of the angular-momentum distribution in the composite system. They can now be expressed as

$$\sigma^2 = \sigma_1^2 + \sigma_2^2 + 2\sigma_{12}^2 \quad (2.20)$$

in terms of the variances σ_k^2 of the angular-momentum distributions of the two fragments and the covariance σ_{12}^2 . The variances approach the equilibrium limit twice as fast as the mean value. This limit becomes

$$\begin{aligned} \sigma_{\text{equ}}^2 &= \frac{\mathcal{J}_1(\mathcal{J}_{\text{rel}} + \mathcal{J}_2)}{\mathcal{J}_{\text{tot}}} T + \frac{\mathcal{J}_2(\mathcal{J}_{\text{rel}} + \mathcal{J}_1)}{\mathcal{J}_{\text{tot}}} T \\ &\quad - 2 \frac{\mathcal{J}_1 \mathcal{J}_2}{\mathcal{J}_{\text{tot}}} T = \frac{\mathcal{J}_{\text{rel}}(\mathcal{J}_1 + \mathcal{J}_2)}{\mathcal{J}_{\text{tot}}} T, \end{aligned} \quad (2.21)$$

which is consistent with results from earlier nonequilibrium⁶ and equilibrium⁵ statistical treatments. The effect of the anticorrelation as expressed by the negative value of the covariance,

$$(\sigma_{12}^2)_{\text{equ}} = - \frac{\mathcal{J}_1 \mathcal{J}_2}{\mathcal{J}_{\text{tot}}} T, \quad (2.22)$$

has been discussed in Ref. 10. For fixed total mass, the absolute value of the covariance reaches a maximum at mass symmetry where it is approximately $\frac{1}{6}$ of σ_1^2 . For asymmetric systems with $\sigma_1^2 \ll \sigma_2^2$

the ratio σ_{12}^2/σ_1^2 can become much larger and a calculation of the angular-momentum distribution of the light fragment critically depends on the effect of the correlation.

We have also considered the correlation angle of the angular-momentum distribution

$$\alpha = \frac{1}{2} \arctan[2\sigma_{12}^2/(\sigma_2^2 - \sigma_1^2)] \quad (2.23)$$

which attains its maximum value of -45° for equal-mass fragments where $\sigma_1^2 = \sigma_2^2$. In the equilibrium limit it becomes

$$\alpha_{\text{equ}} = \frac{1}{2} \arctan \left[- \frac{2\mathcal{J}_1 \mathcal{J}_2}{\mathcal{J}_{\text{rel}}(\mathcal{J}_2 - \mathcal{J}_1)} \right] \quad (2.24)$$

The corresponding correlation coefficient $\chi = \sigma_{12}^2/(\sigma_1 \sigma_2)$ has the equilibrium limit

$$\chi_{\text{equ}} = - \left[1 + \frac{\mathcal{J}_{\text{rel}}^2}{\mathcal{J}_1 \mathcal{J}_2} + \frac{\mathcal{J}_{\text{rel}}}{\mathcal{J}_1} + \frac{\mathcal{J}_{\text{rel}}}{\mathcal{J}_2} \right]^{-1/2} \quad (2.25)$$

These quantities will be calculated in the application of Sec. IV.

Regarding the information that can be derived from γ -multiplicity experiments, the distribution $P(|\vec{I}_1|, |\vec{I}_2|; t)$ of the absolute values of the fragment spins is of interest because the γ multiplicity is not sensitive to the spin direction. Obviously this distribution cannot be Gaussian since it is restricted to positive arguments only. The calculation of the distribution function

$$P(|\vec{I}_1|, |\vec{I}_2|; t) = \int P(\vec{I}_1, \vec{I}_2; t) d\Omega_1 d\Omega_2 \quad (2.26)$$

is tedious but straightforward. We obtain the result

$$\begin{aligned} P(|\vec{I}_1|, |\vec{I}_2|; t) &\equiv P(I_1, I_2; t) = \pi^{-1} d^{-3/2} \eta^{-1} \exp \left[\frac{\xi \cdot \gamma}{\eta} \right] \\ &\quad \times \exp \left[- \frac{1}{2d} (\sigma_2^2 (I_1^2 + \langle I_1^z \rangle^2) + \sigma_1^2 (I_2^2 + \langle I_2^z \rangle^2) - 2\sigma_{12}^2 \langle I_1^z \rangle \langle I_2^z \rangle) \right] \\ &\quad \times 2 \int \frac{\sqrt{\gamma + \eta}}{\sqrt{\gamma - \eta}} \exp \left[\frac{\xi x^2}{\eta} \right] \sinh(x) dx \end{aligned} \quad (2.27)$$

with the abbreviations

$$\begin{aligned} \xi &= d^{-1} (\sigma_1^2 I_2 \langle I_2^z \rangle - \sigma_{12}^2 I_2 \langle I_1^z \rangle), \\ \gamma &= d^{-2} (\sigma_1^4 I_1^2 \langle I_1^z \rangle^2 - 2\sigma_1^2 \sigma_{12}^2 I_1^2 \langle I_1^z \rangle \langle I_2^z \rangle + \sigma_{12}^4 I_1^2 \langle I_2^z \rangle^2 + \sigma_{12}^4 I_1^2 I_2^2), \\ \eta &= 2d^{-2} (\sigma_1^2 \sigma_{12}^2 I_1^2 I_2 \langle I_1^z \rangle - \sigma_{12}^4 I_1 I_2^2 \langle I_2^z \rangle). \end{aligned} \quad (2.28)$$

The remaining one-dimensional integral in (2.27) is performed numerically. The mean values of the distribution

$$\begin{aligned} \langle |\vec{I}_1| \rangle &= \int d^3I_1 d^3I_2 |\vec{I}_1| P(\vec{I}_1, \vec{I}_2; t) \\ &= \int d|\vec{I}_1| d(\vec{I}_2 | I_1^2 I_2^2 | \vec{I}_1) P(|\vec{I}_1|, |\vec{I}_2|; t) \end{aligned} \quad (2.29)$$

and correspondingly $\langle |\vec{I}_2| \rangle$ are obtained as ($k=1,2$)

$$\langle |\vec{I}_k| \rangle = (2\pi)^{-1/2} \sigma_k^{-1} \langle I_k^2 \rangle^{-1} \int_0^\infty x^2 \left\{ \exp \left[-\frac{1}{2\sigma_k^2} (x - \langle I_k^2 \rangle)^2 \right] - \exp \left[-\frac{1}{2\sigma_k^2} (x + \langle I_k^2 \rangle)^2 \right] \right\} dx. \quad (2.30)$$

The sum of the mean values is related to mean γ multiplicities that are accessible experimentally.⁷

A convenient analytical expression of the mean value in the limit of large variances $\langle I_k \rangle^2 \ll \sigma_k^2$ is given by

$$\lim_{\langle I_k \rangle \ll \sigma_k} \langle |\vec{I}_k| \rangle = 2\sqrt{2/\pi} \cdot \sigma_k. \quad (2.31)$$

The variance in the absolute value of the spin of one fragment becomes

$$\sigma_{I_k}^2 \equiv \langle I_k^2 \rangle - \langle |\vec{I}_k| \rangle^2 \quad (2.32)$$

with the limiting value for large fluctuations

$$\lim_{\langle I_k \rangle \ll \sigma_k} \sigma_{I_k}^2 = (3-8|\pi|)\sigma_k^2. \quad (2.33)$$

From (2.33) it is obvious that large statistical fluctuations σ_k^2 of the fragment-spin distribution do not immediately translate into large variances of the absolute values of the spins. It will turn out that the ensuing difficulty⁶ in understanding the experimentally observed⁷ large second moments of γ -multiplicity distributions is not remedied through the consideration of the correlations in the angular momentum distribution. To perform an actual reaction calculation, we sketch the treatment of the relative motion in Sec. III.

III. COUPLING TO THE RELATIVE MOTION

The statistical model for the angular-momentum dissipation outlined above may be coupled to any of the available theories that describe the relative motion of the two ions, such as classical dynamical calculations based on a parametrization of the nucleus-nucleus potential¹⁵ or time-dependent Hartree-Fock calculations.¹⁶ Here we use a phenomenological description of the relative motion that relies on a parametrization of the deflection function rather than the potential. It has been applied to numerous reactions between heavy nuclei where it yields mean total kinetic energy loss, deflection angle, mean angular-momentum loss, and in-

teraction times for each impact parameter.¹⁷

In the expression of the deflection function,

$$\langle \theta(l) \rangle = \theta_R(l) - \beta \theta_{1/4} \frac{l}{l_{gr}} \left[\frac{\delta}{\beta} \right]^{1/l_{gr}}, \quad (3.1)$$

with the Rutherford deflection angle $\theta_R(l)$, the grazing angular momentum

$$l_{gr} \approx 0.22R [A_{red}(E_{c.m.} - V(R_{int}))]^{1/2}$$

and

$$\theta_{1/4} = \theta_R(l_{gr})$$

the two parameters δ, β are monotonic functions of

$$\eta' = Z_1 Z_2 e^2 / v' \quad (3.2)$$

with

$$v' = \left[\frac{2}{\mu} (E_{c.m.} - V(R_{int})) \right]^{1/2}$$

the velocity at the interaction barrier $V(R_{int})$. We have investigated the dependence of β and δ on η' in a comparison with angular distributions for various heavy systems to obtain the approximations

$$\begin{aligned} \beta &= 75f(\eta') + 15, \quad \eta' < 375 \\ &= 36 \exp[-2.17 \times 10^{-3} \eta'], \quad \eta' \geq 375, \\ \delta &= 0.07f(\eta') + 0.11, \quad \eta' < 375 \\ &= 0.117 \exp[-1.34 \times 10^{-4} \eta'], \quad \eta' \geq 375, \end{aligned} \quad (3.3)$$

where

$$f(\eta') = \left[1 + \exp \left[\frac{\eta' - 235}{32} \right] \right]^{-1}.$$

These functions are shown in Fig. 1 together with the values determined from experiment. Minor modifications may be necessary when further reactions are analyzed. The parametrization is not expected to describe very light systems with large fractions of the reaction cross section going into fusion. For sufficiently heavy systems we use it to predict

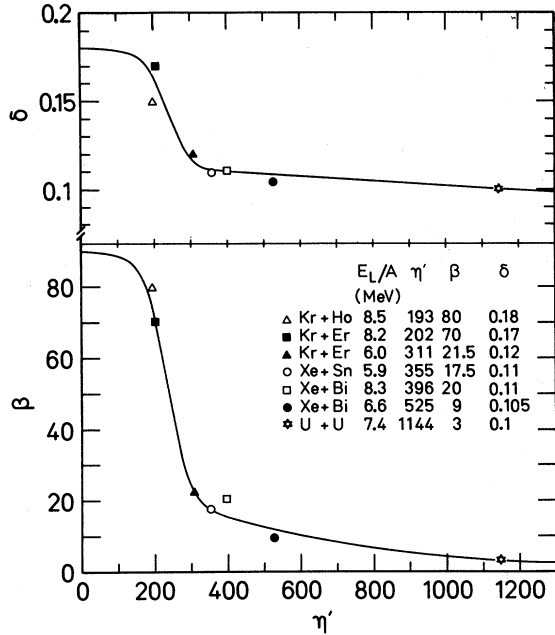


FIG. 1. Parameters β, δ determining the mean deflection angle $\langle \theta(l) \rangle$ as functions of $\eta' = Z_1 Z_2 e^2 / v'$. Symbols represent fits to the angular distributions, the solid curves the analytical expressions given in the text.

the relative-motion information. The resulting deflection function for the Coulomb-dominated system 8.5 MeV/u $^{208}\text{Pb} + ^{238}\text{U}$ is shown as an example in the lower part of Fig. 2. Owing to the large value of η' , both β and δ are small and the resulting deviation from the Rutherford deflection function is also small.

The subsequent calculation of average energy loss, angular-momentum loss, and interaction time has been described in detail in Ref. 17. Here the relaxation times τ_R for radial kinetic energy and τ_ϵ for spheroidal deformations¹⁸ have been determined as

$$\begin{aligned} \tau_R &\simeq 0.3 \times 10^{-21} \text{ s}, \\ \tau_\epsilon &\simeq 4 \times 10^{-21} \text{ s}, \end{aligned} \quad (3.4)$$

and we use these values in the subsequent calculations. The result for the mean total kinetic energy loss as function of the scattering angle is shown in the upper part of Fig. 2. The large energy damping below the interaction barrier reflects the fragment deformation. The description of the average angular-momentum loss from the relative motion is treated in a consistent way with the generation of mean fragment spin as implied by (2.12). Hence the constant angular-momentum relaxation time $\tau_l \simeq 1.5 \times 10^{-21}$ s of Ref. 17 is replaced by

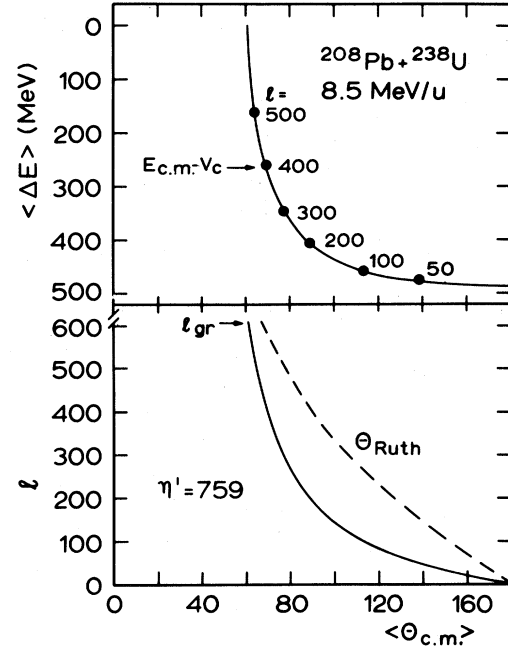


FIG. 2. Correlation between mean energy loss $\langle \Delta E \rangle$ and deflection angle $\langle \theta_{c.m.} \rangle$ as calculated for the reaction 8.5 MeV/u Pb + U. Lower part: deflection function and Rutherford deflection angle.

$$\tau_l = \frac{T^{(l)}}{D_1^{(l)} + D_2^{(l)}} \frac{\mathcal{F}_{\text{rel}}(\mathcal{F}_1 + \mathcal{F}_2)}{\mathcal{F}_{\text{tot}}} \quad (3.5)$$

with the angular-momentum diffusion coefficients $D_k^{(l)}$ that are used in the statistical calculation. They contain a form factor¹⁷ in the large- l region. The mean interaction time $\tau_{\text{int}}(l)$ for given initial relative angular momentum l is calculated as in Ref. 17.

IV. APPLICATIONS

The results of our statistical model of Sec. II for the angular-momentum dissipation can now be evaluated with the help of Sec. III as a function of initial relative angular momentum l or energy loss ΔE . The mean value of the energy loss is a monotonic function of l as shown in Fig. 3 for both fragments $k = 1, 2$ in the $^{208}\text{Pb} + ^{238}\text{U}$ reaction discussed above. The mean value of the dissipated angular momentum in both fragments already approaches the sticking limit at comparatively large values of l for a saturation value of the angular-momentum diffusion coefficient

$$D_l = 20 \times 10^{22} \text{ s}^{-1}. \quad (4.1)$$

This value has been chosen on the basis of the

analysis⁶ for other systems, and the microscopic model of Ayik *et al.*⁶ It may have to be adjusted when the data become available. We have divided D_I according to the fragment-mass ratio in order to obtain the angular-momentum diffusion coefficients D_1, D_2 referred to in Sec. II.

In Fig. 3 we also exhibit the variances of the angular-momentum distributions in both fragments, together with the corresponding covariance, correlation coefficient, and correlation angle. As discussed in Ref. 10, the latter quantities become negative since the angular-momentum distributions in the two fragments are anticorrelated.

The impact-parameter dependent quantities of Fig. 3 provide the ingredients for the calculation of the angular-momentum distribution functions for various mean total kinetic energy losses $\langle \Delta E \rangle$. As functions of the z components I_1, I_2 of the intrinsic angular momenta, $P(I_1, I_2; \langle \Delta E \rangle)$ is Gaussian. The mean values $\langle I_1 \rangle, \langle I_2 \rangle$ first rise as the energy loss increases but then fall towards zero since the largest energy loss corresponds to small initial relative angular momenta and consequently small values of $\langle I_k \rangle$. The distribution function $P(|\vec{I}_1|, |\vec{I}_2|; \langle \Delta E \rangle)$ exhibits a completely different behavior. It is constrained to the positive domain and hence is not Gaussian, as discussed in Sec. II. The mean values $\langle |\vec{I}_k| \rangle$ first rise as the energy loss increases, but then they remain large and

almost constant in the completely damped regime shown in Fig. 4. The fluctuations of the spin in the heavier fragment are larger than the ones in the light fragment, essentially due to the larger moment of inertia. We have restricted the calculation to fragments of the entrance-channel mass asymmetry. It would certainly be of interest if these distribution functions could be measured in the future.

In Fig. 5 we display the mean values $\langle |\vec{I}_k| \rangle$ for both fragments $k=1,2$ as functions of the initial relative angular momentum l . Their insensitivity to l in a broad range is the underlying reason for the independence on energy loss in the completely damped regime. The alignment of the respective fragments,

$$P_{zz}^{(k)} = \frac{3}{2} \left\langle \frac{I_k^{(z)2}}{I_k^2} \right\rangle - \frac{1}{2}, \quad (4.2)$$

is shown in Fig. 5 in the approximation⁶

$$P_{zz}^{(k)} \simeq \frac{3}{2} \frac{\langle I_k^{(z)2} \rangle}{\langle I_k^2 \rangle} - \frac{1}{2} = \frac{3}{2} \frac{\langle I_k \rangle^2 + \sigma_k^2}{\langle I_k \rangle^2 + 3\sigma_k^2} - \frac{1}{2}, \quad (4.3)$$

which is valid for the Gaussian distribution functions of Sec. II. Obviously the alignment is very sensitive to the model assumptions used for the calculation of the in-plane fluctuations. As a consequence of the simplifications described in Sec. II, the fluctuations in the three spatial directions are equal, such that the alignment values shown in Fig. 5 are expected to represent lower limits.

The results of Fig. 6 for the system $^{86}\text{Kr} + ^{154}\text{Sm}$ at bombarding energies 5.7 and 7 MeV/u may be compared to available data.¹¹ The calculation proceeds as described for Pb + U, but the angular-momentum diffusion coefficients have the smaller values of

$$\begin{aligned} D_I(5.7 \text{ MeV/u}) &= 7 \times 10^{22} \text{ s}^{-1}, \\ D_I(7 \text{ MeV/u}) &= 10 \times 10^{22} \text{ s}^{-1}, \end{aligned} \quad (4.4)$$

which have now been determined according to the comparison with the measured γ -multiplicity values.¹¹ In the upper part of Fig. 6 we show the calculated energy spectra

$$\frac{d\sigma}{dE} = \frac{2\pi}{K^2} \int_0^{l_{\max}} l P(\Delta E, \tau_{\text{int}}(l)) dl \quad (4.5)$$

integrated over all fragments and scattering angles. At both energies they extend well below the barrier. The Gaussian distribution function $P(\Delta E, t)$ has an impact-parameter dependent mean value calculated as in Ref. 18. The variance in energy loss for a given initial relative angular momentum is

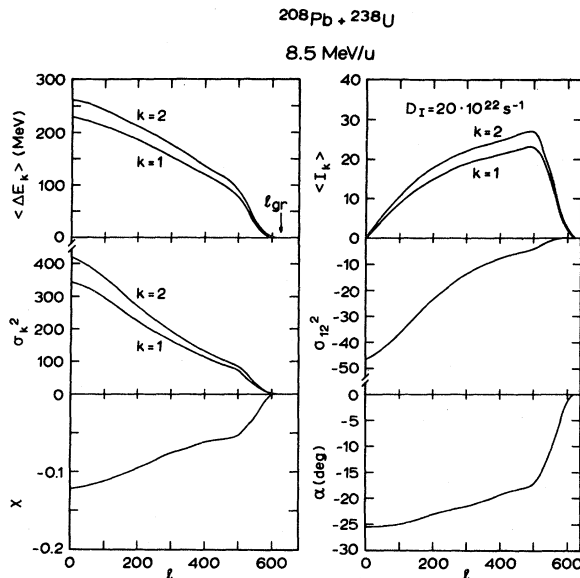


FIG. 3. Average energy- and angular-momentum loss for both fragments $k=1,2$ in the 8.5 MeV/u $^{208}\text{Pb} + ^{238}\text{U}$ collision, together with variances σ_k^2 , covariance σ_{12}^2 , correlation coefficient χ , and correlation angle α of the angular-momentum distribution.

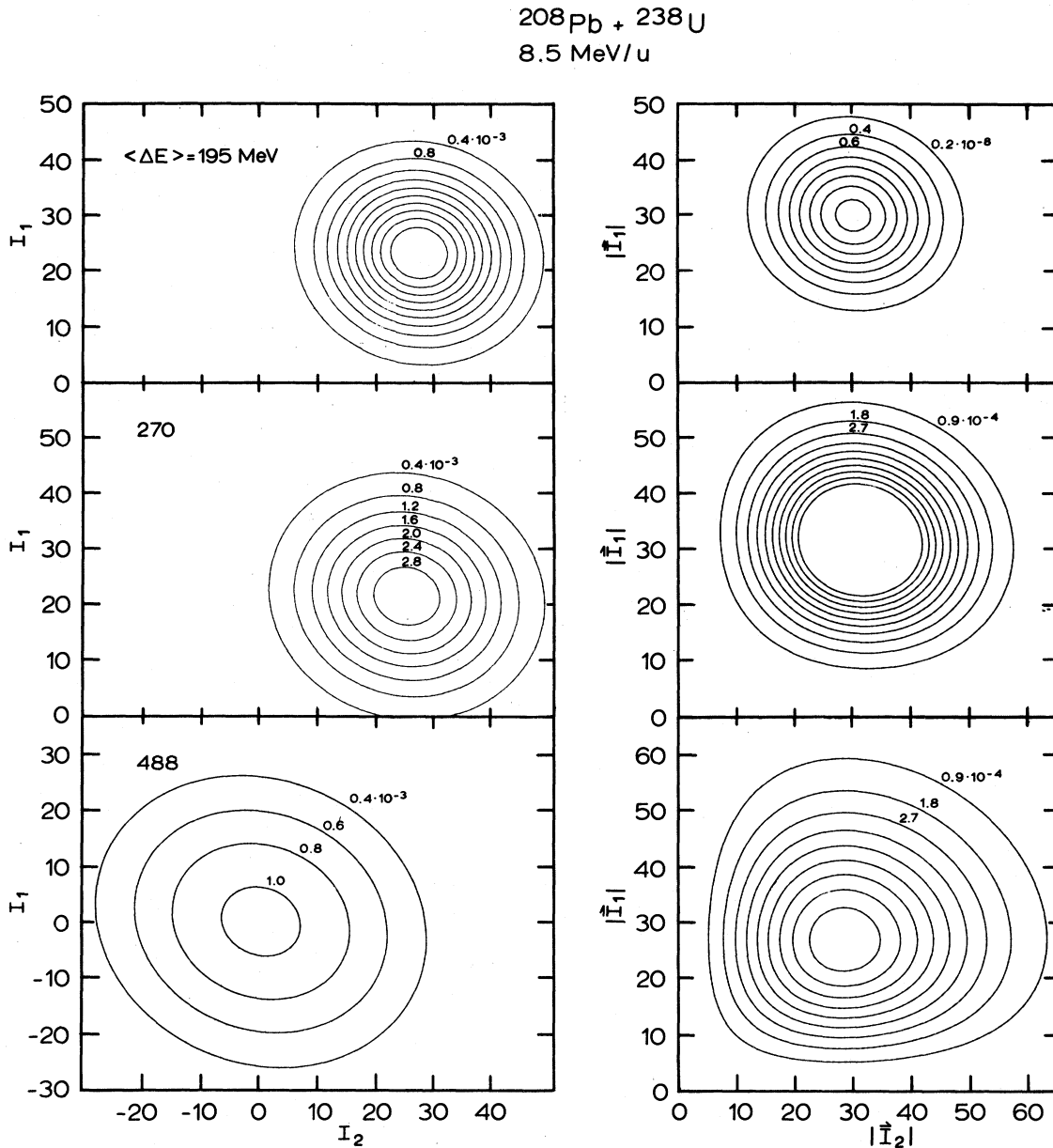


FIG. 4. Contour plots of distributions $P(I_1, I_2; \tau_{\text{int}})$ for the z components of the intrinsic angular momenta (lhs) and $P(|\vec{I}_1|, |\vec{I}_2|; \tau_{\text{int}})$ for the absolute values (rhs). Results for three different values of the mean energy loss $\langle \Delta E \rangle$ are shown.

represented by

$$\sigma_E^2 = 2\Delta E_{\text{rad}}^{(l)} T^{(l)}, \quad (4.6)$$

where $\Delta E_{\text{rad}}^{(l)}$ is the loss of radial energy for each l value. For the reaction 7 MeV/u $^{86}\text{Kr} + ^{154}\text{Sm}$, this corresponds to an upper limit in the FWHM of the energy loss of

$$\Gamma_{\text{FWHM}}^E \leq (8 \ln 2)^{1/2} \times 28.2 \text{ MeV} \simeq 66 \text{ MeV}. \quad (4.7)$$

The value (4.6) has not been chosen on theoretical grounds although one might justify it on the basis of a diffusion equation for the energy loss. In a comparison of calculated energy spectra with experimen-

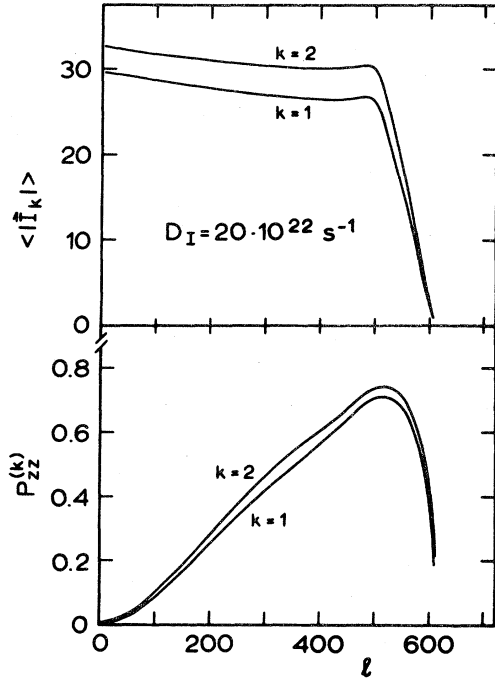


FIG. 5. Mean absolute values of the intrinsic angular momenta for both fragments and fragment-spin alignment P_{zz} as functions of the initial angular momentum l in the Pb + U reaction.

tal results for several heavy systems the ansatz (4.5) yields good agreement in the tails of the energy spectra, whereas energy-loss fluctuations that are calculated from the shape fluctuations at scission only¹⁸ are consistently too small.

The mean absolute values of the dissipated angular momentum are shown in the middle part of Fig. 6 as functions of energy loss. Their sum is compared to the γ -multiplicity data of Christensen *et al.*¹¹ The scale on the right-hand side (rhs) refers to the data. The conversion shown in the figure corresponds to

$$\langle |\vec{I}_1| \rangle + \langle |\vec{I}_2| \rangle = 2\langle M_\gamma \rangle - 10. \quad (4.8)$$

We attribute the discrepancies between data and calculations in the low-energy loss regime mainly to the fact that this conversion should be energy dependent. However, a careful investigation of the energy dependence of (4.8) does not appear to be available. The data are well reproduced in the completely damped region. Experimental information concerning the individual fragments is not available.

The lower part of Fig. 6 shows the calculated fluctuations in the distributions of the absolute values of the dissipated angular momentum in the two fragments together with their sum. It gives an

upper limit to the variance of the (correlated) distribution $P(|\vec{I}_1| + |\vec{I}_2|)$ of the sum of the spins. The projected distributions $P(|\vec{I}_1|)$, $P(|\vec{I}_2|)$ are shown in Fig. 7 together with their sum for a fixed value of the total kinetic energy loss. Its variance is the quantity that should be compared to the second moment of γ -multiplicity distributions which do not distinguish the fragments. Experimental results for the ratio between standard deviation and mean obtained from the γ -multiplicity distribution are¹¹ $\sigma/\langle |\vec{I}| \rangle \simeq 0.45$ for 5.7 MeV/u and 0.37 for 7 MeV/u $^{86}\text{Kr} + ^{154}\text{Sm}$. The theoretical values as obtained from Fig. 6 are smaller, $\sigma/\langle |\vec{I}| \rangle \simeq 0.32$ and 0.29 for the respective two energies. Again the comparison between theory and experiment crucially depends on the conversion between angular momentum and γ -multiplicity values, but the underestimate of the experimental second moments in the calculation⁶ persists when the correlated angular-momentum distributions are considered. It is noted that the variance provided by the triangular distribution of initial l values should not be added to the theoretical values calculated here. The various l values contributing to a given energy loss have already been taken into account since the fluctuations in energy loss are included in an *ad hoc* but realistic way.

V. CONCLUSIONS

We have calculated angular-momentum distributions for both fragments in deeply inelastic heavy-ion collisions. A nonequilibrium-statistical model has been given and analytical results for the distribution functions of the angular momenta and their absolute values have been derived. Expressions for mean values and variances of the spin of both fragments and their absolute values have been calculated. The latter are relevant in comparison with γ -multiplicity experiments. However, experimental results which discriminate between the two fragments are not yet available.

In conjunction with a phenomenological model for the description of the relative motion we have applied the results of our statistical treatment to the reactions 8.5 MeV/u $^{208}\text{Pb} + ^{238}\text{U}$ as well as 5.7 MeV/u and 7 MeV/u $^{86}\text{Kr} + ^{154}\text{Sm}$. For the Kr + Sm system, experimental results for the sum of the γ multiplicity from both fragments exist.^{7,11} The mean values of the calculated distribution as a function of energy loss are consistent with the data whereas the standard deviations of the correlated distribution functions appear to be too small. A systematic comparison with a large set of data at different bombarding energies could clarify the origin of the disagreement, together with investigations of

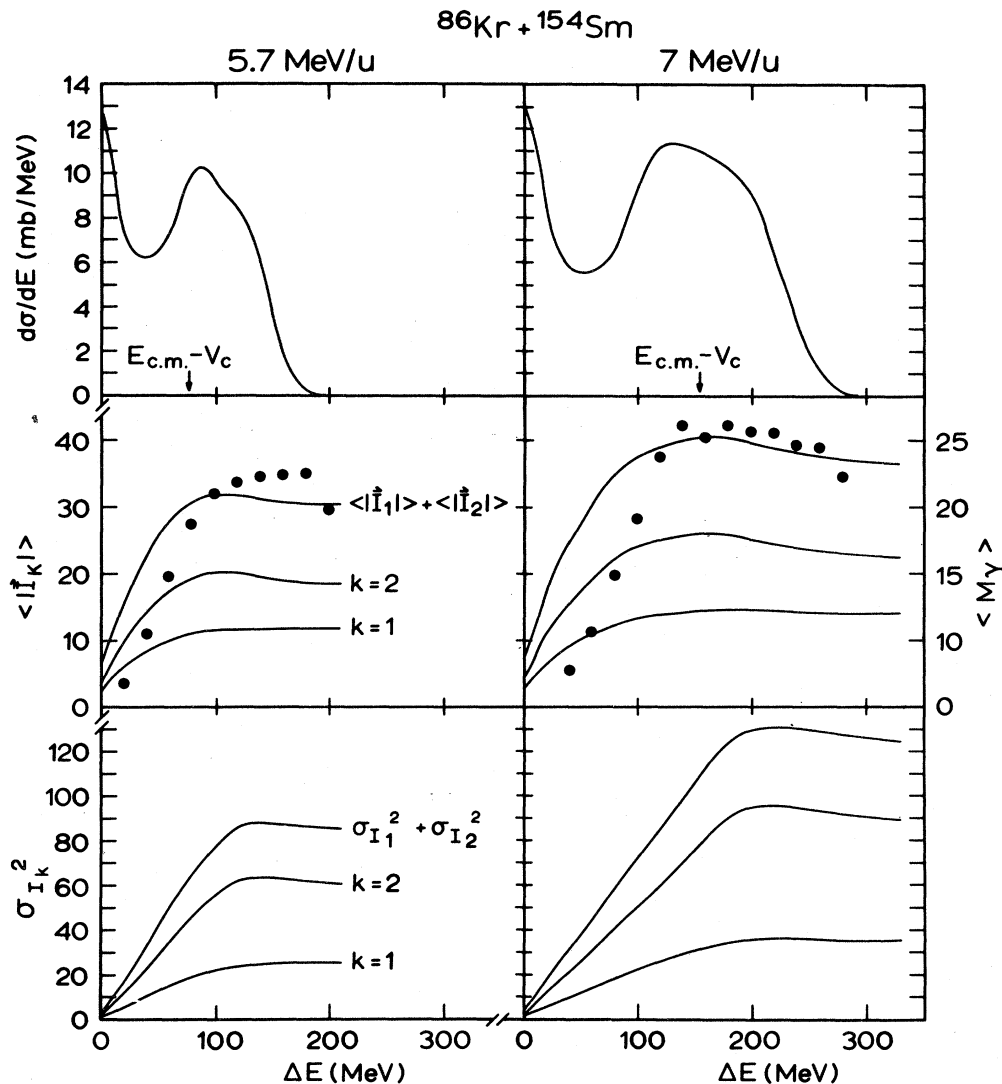


FIG. 6. Energy spectra, mean value, and variance of the dissipated angular momentum in the Kr + Sm reaction at two different bombarding energies. Data points from the γ -multiplicity experiments of Ref. 11 refer to the scale of the rhs.

the relation between spin and γ multiplicity and its energy-loss dependence.

To provide the analytical treatment outlined in this work several approximations, especially concerning the diffusion tensor, have been unavoidable. The angular-momentum diffusion coefficients corresponding to the two fragments are taken to be constant for each initial l value, and a distinction of components in the spatial directions is not made. As a consequence, we cannot describe differences in the components of the in-plane fluctuations. This certainly limits our description of the angular-momentum transport, especially at large mass asymmetries. Numerical solution schemes of the trans-

port equation which allow for a more complicated structure of the diffusion tensor are necessary to deal with the differences in the in-plane fluctuations. This will provide more realistic values for the spin alignment and alignment correlations between the two fragments, whereas our calculation yields a lower limit for $P_{zz}^{(k)}$. The comparison with alignment data for the fissioning fragment¹⁹ or both fragments in double-sequential fission experiments may require a refined treatment of the in-plane fluctuations. It might also be of interest to investigate the influence of the mixed components of the diffusion tensor on the correlations of the fragment spins.

Another topic of considerable interest which we

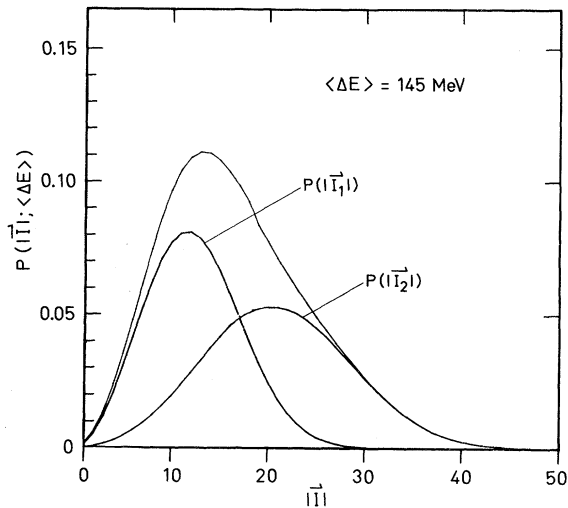


FIG. 7. Projected angular-momentum distributions $P(|\vec{I}_1|)$, $P(|\vec{I}_2|)$, and $P(|\vec{I}_1|) + P(|\vec{I}_2|)$ for 7 MeV/u Kr + Sm at a mean total kinetic energy loss of 145 MeV.

have not investigated is the dependence of the transferred angular momentum and its fluctuations on the fragment-mass asymmetry.^{1,5-17,11,20} The increase of γ -multiplicity values toward mass symmetry found in Ref. 20 reflects the rise of the statistical components. This effect can be treated by coupling a diffusion equation for the mass-asymmetry mode to the transport equation for the angular-momentum dissipation. Regarding the observables that we have calculated, it will be of interest to deduce experimental information on mean values and variances of the angular-momentum distribution in both fragments, and eventually measure the two-dimensional distribution function.

ACKNOWLEDGMENTS

We gratefully acknowledge discussions with T. Døssing, H. Freiesleben, A. Lazzarini, and U. Lynen, and we thank X. T. Tang for contributions in the early stages of this work. This work was supported by the Deutsche Forschungsgemeinschaft.

*Permanent address: Institute of Modern Physics, Lanzhou, China.

¹M. Lefort and C. Ngô, Riv. Nuovo Cimento **2**, 1 (1979).

²H. A. Weidenmüller, Prog. Part. Nucl. Phys. **3**, 49 (1980).

³W. Nörenberg, Phys. Lett. **52B**, 289 (1974); A. Gobbi and W. Nörenberg in *Heavy-Ion Collisions*, edited by R. Bock (North-Holland, Amsterdam, 1980), Vol. 2.

⁴W. Albrecht, W. Dünnweber, G. Graw, H. Ho, S. G. Steadman, and J. P. Wurm, Phys. Rev. Lett. **34**, 1400 (1975); G. Wolschin, in *Nuclear Structure and Heavy-Ion Collisions, LXXVII Corso Varenna*, edited by R. A. Broglia, R. A. Ricci, and C. H. Dasso (Soc. Italiana di Fisica, 1981), p. 507.

⁵L. G. Moretto, Ref. 4, p. 85; L. G. Moretto and R. P. Schmitt, Phys. Rev. C **21**, 204 (1980); L. G. Moretto, S. K. Blau, and A. J. Pacheco, Nucl. Phys. **A364**, 125 (1981); A. J. Pacheco, and L. G. Moretto, Z. Phys. A **306**, 259 (1982).

⁶G. Wolschin, Fizika **9**, 513 (1977); Nucl. Phys. **A316**, 146 (1979); S. Ayik, G. Wolschin, and W. Nörenberg, Z. Phys. A **286**, 271 (1978); G. Wolschin and W. Nörenberg, Phys. Rev. Lett. **41**, 691 (1978).

⁷P. R. Christensen, F. Folkmann, Ole Hansen, O. Nathan, N. Trautner, F. Videbaek, S. Y. van der Werf, H. C. Britt, R. P. Chestnut, F. Freiesleben, and F. Pühlhofer, Phys. Rev. Lett. **40**, 1245 (1978); A. Olmi, H. Sann, D. Pelte, Y. Eyal, A. Gobbi, W. Kohl, U. Lynen, G. Rudolf, H. Stelzer, and R. Bock, *ibid.* **41**, 688 (1978); R. Regimbart, A. N. Behkami, G. L. Wozniak, R. P. Schmitt, J. S. Sventek, and L. G. Moretto, *ibid.* **41**,

1355 (1978).

⁸R. J. Puigh, P. Dyer, R. Vandenbosch, T. D. Thomas, L. Nunnelley, and M. S. Zisman, Phys. Lett. **86B**, 24 (1979); G. J. Wozniak, R. J. McDonald, A. J. Pacheco, C. C. Hsu, D. J. Morrissey, L. G. Sobotka, L. G. Moretto, S. Shih, C. Schuck, R. M. Diamond, H. Kluge, and F. S. Stephens, Phys. Rev. Lett. **45**, 1081 (1980); R. J. Puigh, H. Doubré, A. Lazzarini, A. Seamster, R. Vandenbosch, M. S. Zisman, and T. D. Thomas, Nucl. Phys. **A336**, 279 (1980).

⁹D. v.Harrach, P. Glässel, Y. Civelekoglu, R. Männer, and H. J. Specht, Phys. Rev. Lett. **42**, 1728 (1979).

¹⁰J. Q. Li, X. T. Tang, and G. Wolschin, Phys. Lett. **105B**, 107 (1981); Phys. Ener. For. Phys. Nucl. (Lanzhou) **6**, 341 (1982).

¹¹P. R. Christensen, F. Folkmann, Ole Hansen, O. Nathan, N. Trautner, F. Videbaek, and S. Y. van der Werf, Nucl. Phys. **A349**, 217 (1980); P. R. Christensen, Ole Hansen, O. Nathan, F. Videbaek, H. Freiesleben, H. C. Britt, and S. Y. van der Werf (unpublished).

¹²A. Lazzarini, private communication.

¹³J. Randrup, Lawrence Berkeley Laboratory Report LBL-12676, 1981.

¹⁴R. A. Broglia, G. Pollarolo, C. H. Dasso, and T. Døssing, Phys. Rev. Lett. **43**, 1649 (1979).

¹⁵D. H. E. Gross and H. Kalinowski, Phys. Lett. **C45**, 177 (1978); K. Siwek-Wilczyńska, J. Wilczyński, Nucl. Phys. **A264**, 115 (1976); C. Ngô, H. Hofmann, Z. Phys. A **282**, 83 (1977); R. Schmidt, V. D. Toneev, and G. Wolschin, Nucl. Phys. **A311**, 247 (1978); F. Beck, J. Blocki, M. Dworzecka, G. Wolschin, Phys. Lett. **76B**,

- 35 (1978); J. Blocki, M. Dworzecka, F. Beck, and H. Feldmeier, *ibid.* 29B, 13 (1981).
- ¹⁶K. T. R. Davies, K. R. S. Devi, S. E. Koonin, and M. R. Strayer, California Institute of Technology Report No. Map-23, 1982, and references contained therein.
- ¹⁷G. Wolschin, *Nukleonika* 22, 1165 (1977); G. Wolschin and W. Nörenberg, *Z. Phys. A* 284, 209 (1978); C. Riedel, G. Wolschin, and W. Nörenberg, *ibid.* 290, 47 (1979).
- ¹⁸G. Wolschin, *Phys. Lett.* 88B, 35 (1979).
- ¹⁹T. Døssing, *Nucl. Phys.* A357, 488 (1981).
- ²⁰R. Bock, Y. T. Chu, M. Dakowski, A. Gobbi, E. Grosse, A. Olmi, H. Sann, D. Schwalm, U. Lynen, W. Müller, S. Bjørnholm, H. Esbensen, W. Wölfli, and E. Morenzoni, *Nucl. Phys.* (to be published).